National Physical Laboratory

NPL REPORT TQE 12

Commissioning of the NPL WR-05 Waveguide Network Analyser System for S-Parameter Measurements from 140 GHz to 220 GHz

N Shoaib, N M Ridler and M J Salter

MARCH 2015

Commissioning of the NPL WR-05 Waveguide Network Analyser System for S-Parameter Measurements from 140 GHz to 220 GHz

N Shoaib[1], N M Ridler and M J Salter
Time, Quantum and Electromagnetics Division

ABSTRACT

This report describes some investigations into the performance of the new NPL Vector Network Analyser (VNA) system in terms of scattering parameter (S-parameter) measurements from 140 to 220 GHz. Two types of investigation have been undertaken: (a) connection repeatability; and (b) a comparison of different calibration techniques.

(a) For the connection repeatability investigation, four one-port devices were used: (i) a flush short-circuit; (ii) an offset short-circuit; (iii) a near-matched termination; and (iv) a mismatched termination. The experimental standard deviation was computed and used as the measure of variability in the measurement results due to flange connection repeatability. The repeatability analysis was performed separately on the real and imaginary components of the complex-valued linear voltage reflection coefficient (VRC). Isolation measurements, providing an indication of the VNA 'noise floor' for transmission measurements, were also made as part of this investigation.

(b) For the comparison of the calibration techniques, several two-port calibration techniques were implemented using the available WR-05 waveguide standards. Two different classes of calibration technique were implemented: (i) three known one-port devices and a thru (i.e. the three-known-loads-thru (TKLT) technique); (ii) the Thru-Reflect-Line (TRL) and Line-Reflect-Line (LRL) techniques. A wide range of one- and two-port devices under test (DUTs) were measured during the comparison. Mechanical length measurements were also made on some of the one- and two-port DUTs. These length measurements have been used subsequently to compare with electrical length computations obtained using measurements from the different calibration techniques.

[1] NPL Visiting Researcher from Department of Electronics and Communications, Politecnico Di Torino, Italy.

ISSN 1754-2995

National Physical Laboratory
Hampton Road, Teddington, Middlesex, TW11 0LW

Approved on behalf of NPL Management Ltd by Dr Rhys Lewis, Division Head – Time, Quantum and Electromagnetics Division.

CONTENTS

1. INTRODUCTION

In high-frequency electronics engineering, the Vector Network Analyser (VNA) is one of the most versatile, multi-functional, measuring instruments used for electronic component and circuit analysis. In recent years, VNAs have been developed that enable measurements to be made at millimetre-wave frequencies and above (specifically, at frequencies above 110 GHz). These VNAs use rectangular metallic waveguide test ports via external waveguide extenders to perform the measurements. However, at these frequencies, the dimensions of the waveguide aperture become very small. Therefore, accurate and repeatable dimensional alignment of the waveguide becomes very important in order to achieve reliable and repeatable scattering parameter (S-parameter) measurements. A slight misalignment of the waveguide will give rise to reflections at the interface between two connected waveguides. This misalignment will cause systematic and random errors in the electrical measurements. Therefore, it is important to evaluate the connection repeatability performance due to the waveguide flanges' alignment mechanisms.

Along with connection repeatability, it is also informative to compare, from a metrological point of view, different VNA calibration techniques at millimetre-wave frequencies. The VNA calibration is a procedure that characterises the measurement system's systematic errors and then subsequently removes these errors mathematically from the measurements. The calibration procedure also defines the reference planes for the measurement test ports. Each calibration procedure uses a particular set of calibration standards. Two different classes of calibration technique are used to calibrate a two-port VNA: (i) using three known loads and a thru connection; and (ii) Thru-Reflect-Line (TRL) and Line-Reflect-Line (LRL).

This report describes a detailed investigation into the performance of the new NPL WR-05 waveguide VNA capability for S-parameter measurements from 140 GHz to 220 GHz. The report is in two parts. The first part is dedicated to a connection repeatability investigation while the second part describes a comparison of different two-port calibration techniques.

2. CONNECTION REPEATABILITY INVESTIGATION

The connection repeatability investigation used four one-port devices under test (DUT): a flush short-circuit, an offset short-circuit, a near-matched termination and a mismatched termination. These devices can be used as standards for calibrating VNAs. In order to evaluate the connection repeatability, the measurement of each DUT was repeated 10 times under essentially the same conditions of measurement (i.e. under repeatability conditions [1]).

Before performing the repeatability investigation, an assessment was made of the VNA isolation. The isolation assessment provides information about the cross-talk between the test ports. The isolation measurements are also presented here.

This section of the report is organised as follows: section 2.1 describes the experimental set-up; section 2.2 describes the statistical techniques used for the data analysis; section 2.3 presents the results of the analysis; and, section 2.4 contains a discussion of the results.

2.1 EXPERIMENTAL SETUP

The measurements were made using NPL's new 67 GHz four-port Agilent Technologies PNA-X network analyser, model N5247A (NPL reference name 'Unit 17'). Two Virginia Diodes, Inc (VDi) WR-05 millimetre-wave extenders, models VNAX239 and VNAX240, were used to extend the frequency range of the VNA to cover from 140 GHz to 220 GHz. Measurements were carried out in NPL Laboratory F2-L11 that has stable room temperature (23 °C ± 2 °C). The measurement set-up is shown in Fig. 1.

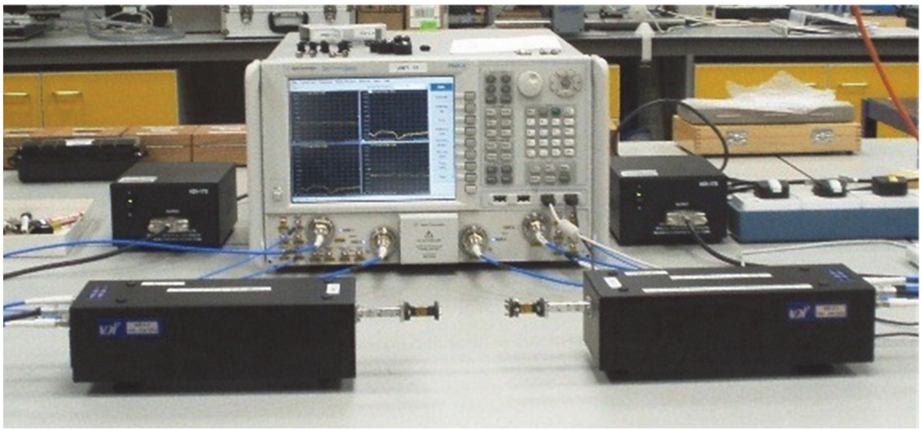

Figure 1: VNA measurement set-up used in NPL laboratory F2-L11

The VNA was calibrated using a one-port three-known-loads calibration technique [2]-[6]. For waveguide measurements, it is not straightforward to realise an open-circuit standard (due to difficult-to-quantify radiation effects at the open end of the waveguide) so an offset short was used (in place of the open-circuit) as one of the known loads. The calibration was made using the VDi WR-05 calibration kit (NPL Reference CIS/C/904). The calibration standards used for performing the VNA calibration are shown in Table 1. The DUTs used for the investigation are shown in Table 2.

Table 1: Calibration standards

Calibration Standard	Manufacturer	NPL calibration kit ID
Flush Short	Virginia Diodes, Inc. (VDi)	CIS/C/904
Offset (Quarter Wavelength) Short	Virginia Diodes, Inc. (VDi)	CIS/C/904
Near-matched Load	Virginia Diodes, Inc. (VDi)	CIS/C/904

Table 2: DUTs used for the repeatability investigation

Device	Manufacturer	Serial Number	NPL calibration kit ID
Flush Short	Virginia Diodes, Inc. (VDi)	SC 2-54	CIS/C/904
Offset Short	Flann Microwave	177977	CIS/C/902
Near-matched Termination	Flann Microwave	177714	CIS/C/902
Mismatched Termination	Flann Microwave	177962	CIS/C/902

2.2 DATA ANALYSIS

The experimental standard deviation [7] was used to quantify the variability in the measurement results due to flange connection repeatability. Since the measurement results are complex-valued quantities the standard deviation computation is applied separately to the real and imaginary components of the complex-valued linear voltage reflection coefficient.

Let Γ be the complex-valued measured reflection coefficient with Γ_R and Γ_I being the real and imaginary components of Γ, respectively. Γ can be written as follows:

$$\Gamma = \Gamma_R + j\Gamma_I \quad (1)$$

where $j^2 = -1$. For n repeat measurements of Γ, the mean value of Γ_R can be computed as follows:

$$\overline{\Gamma}_R = \frac{1}{n}\sum_{k=1}^{n}\Gamma_{R_k} \qquad (2)$$

and the experimental standard deviation of Γ_R can be expressed as follows:

$$s(\Gamma_R) = \sqrt{\frac{1}{n-1}\sum_{m=1}^{n}(\Gamma_{R_m} - \overline{\Gamma}_R)^2} \qquad (3)$$

Similarly, the mean value of Γ_I can be computed as follows:

$$\overline{\Gamma}_I = \frac{1}{n}\sum_{k=1}^{n}\Gamma_{I_k} \qquad (4)$$

and the experimental standard deviation of Γ_I can be expressed as follows:

$$s(\Gamma_I) = \sqrt{\frac{1}{n-1}\sum_{m=1}^{n}(\Gamma_{I_m} - \overline{\Gamma}_I)^2} \qquad (5)$$

In our case, since each DUT is measured 10 times at each frequency, $n = 10$. The $s(\Gamma_R)$ and $s(\Gamma_I)$ values are computed at each frequency using the 10 repeated measurements of each DUT.

The experimental standard deviation calculations, presented in this section of the report, were made using Equations (1) to (5). Results from an alternative method of calculating the experimental standard deviation [8] for the near-matched termination and offset short-circuit are also presented in the Appendix.

2.3 MEASUREMENT RESULTS

2.3.1 Isolation measurements

The isolation assessment was carried out by terminating the two test ports with short-circuits and measuring the transmission coefficients, S_{12} and S_{21}. These results, shown in Figure 2, indicate that the isolation achieved by the VDi Extender Heads is better than –110 dB across the whole waveguide band. This is considered to represent very good isolation performance for this waveguide band.

2.3.2 Flush short-circuit measurements

Computed values of $s(\Gamma_R)$ and $s(\Gamma_I)$ for the flush short-circuit are shown in Figure 3. Selected values, taken at equally-spaced frequencies across the band, are also presented in Table 3.

2.3.3 Offset short-circuit measurements

Computed values of $s(\Gamma_R)$ and $s(\Gamma_I)$ for the offset short-circuit are shown in Figure 4. Selected values, taken at equally spaced frequencies across the band, are also presented in Table 4.

2.3.4 Near-matched termination measurements

Computed values of $s(\Gamma_R)$ and $s(\Gamma_I)$ for the near-matched termination are shown in Figure 5. Selected values, taken at equally spaced frequencies across the band, are also presented in Table 5.

2.3.5 Mismatched termination measurements

Computed values of $s(\Gamma_R)$ and $s(\Gamma_I)$ for the mismatched termination are shown in Figure 6. Selected values, taken at equally spaced frequencies across the band, are also presented in Table 6.

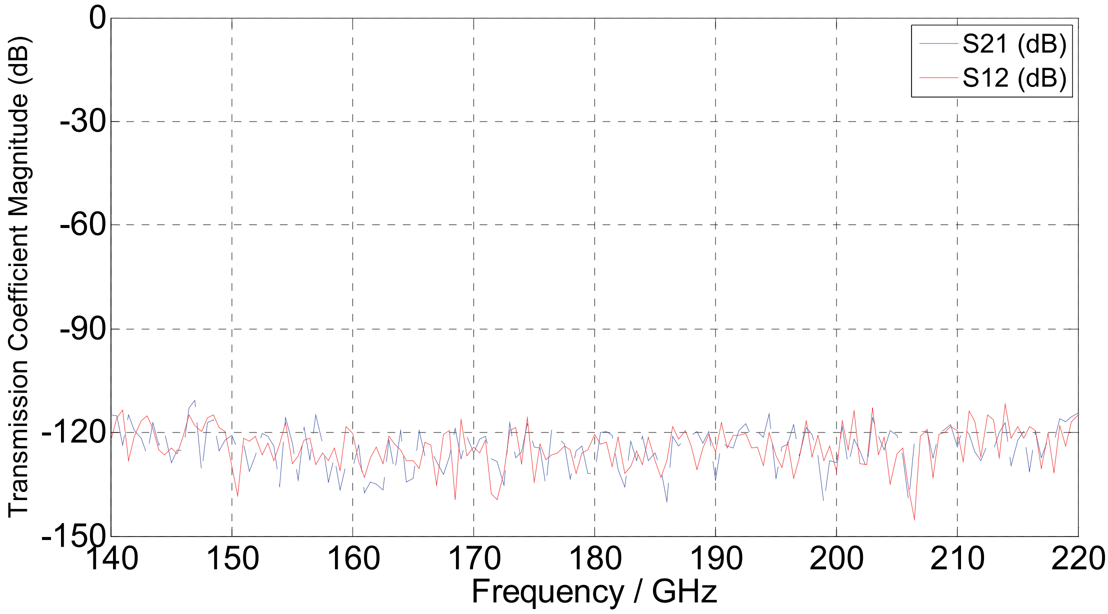

Figure 2: Isolation assessment results

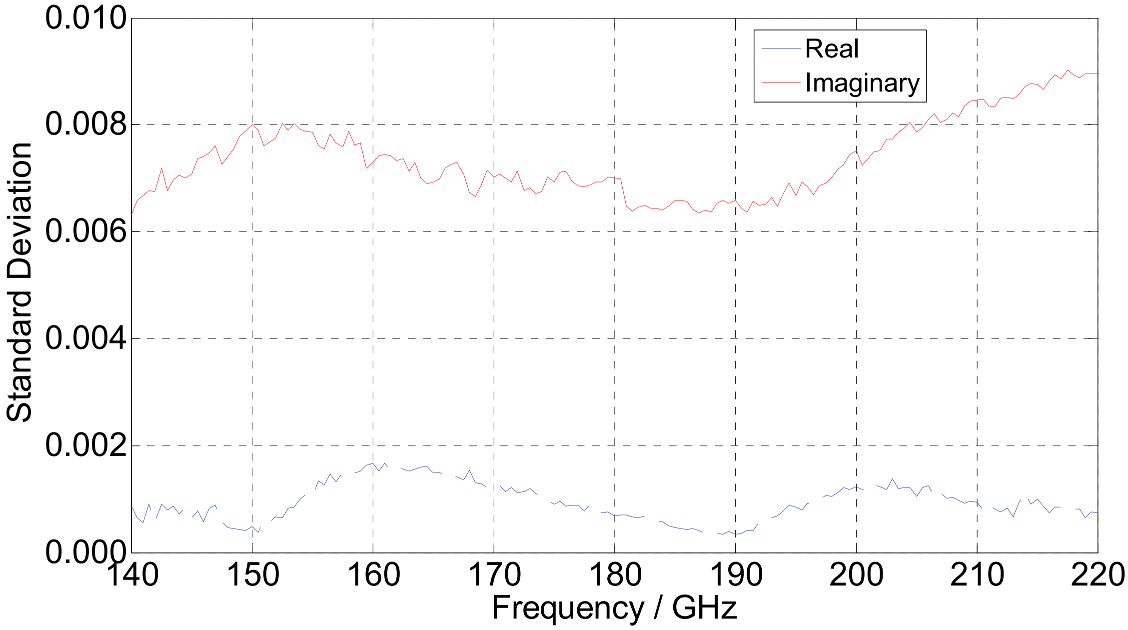

Figure 3: $s(\Gamma_R)$ and $s(\Gamma_I)$ values for the flush short-circuit

Table 3: $s(\Gamma_R)$ and $s(\Gamma_I)$ values for the flush short-circuit at selected frequencies

Frequency (GHz)	$s(\Gamma_R)$	$s(\Gamma_I)$
140	0.0009	0.0063
160	0.0017	0.0073
180	0.0007	0.0070
200	0.0012	0.0075
220	0.0007	0.0090
Average	0.0010	0.0074

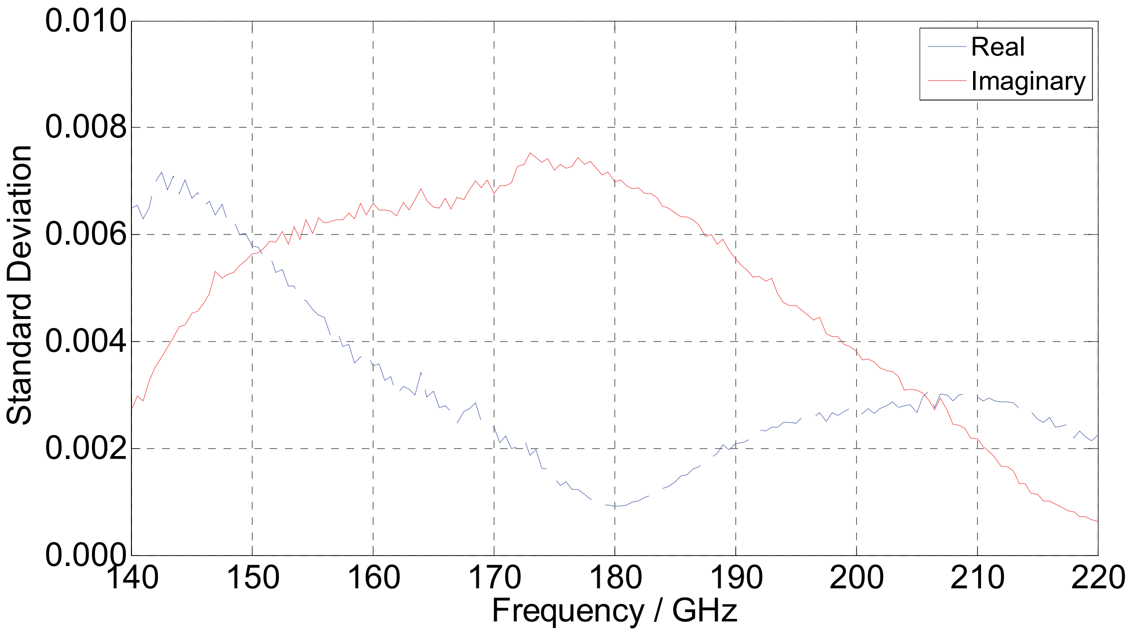

Figure 4: $s(\Gamma_R)$ and $s(\Gamma_I)$ values for the offset short-circuit

Table 4: $s(\Gamma_R)$ and $s(\Gamma_I)$ values for the offset short-circuit at selected frequencies

Frequency (GHz)	$s(\Gamma_R)$	$s(\Gamma_I)$
140	0.0065	0.0027
160	0.0035	0.0066
180	0.0009	0.0070
200	0.0026	0.0038
220	0.0022	0.0006

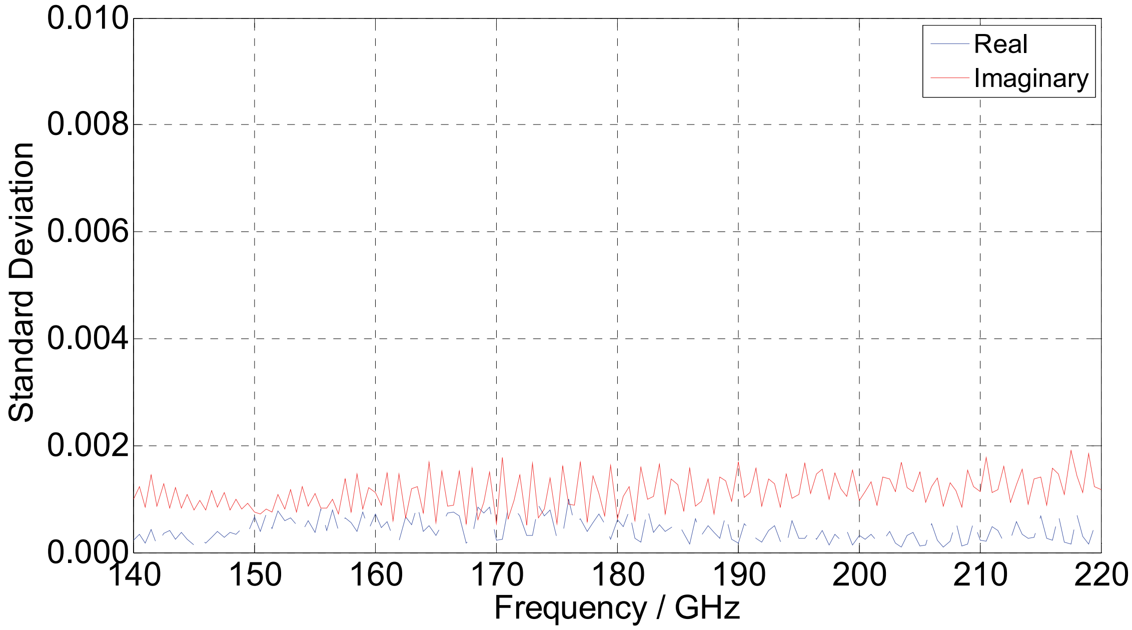

Figure 5: $s(\Gamma_R)$ **and** $s(\Gamma_I)$ **values for the near-matched termination**

Table 5: $s(\Gamma_R)$ **and** $s(\Gamma_I)$ **values for the near-matched termination at selected frequencies.**

Frequency (GHz)	**s(Γ*R*)**	**s(Γ*I*)**
140	0.0002	0.0010
160	0.0007	0.0011
180	0.0006	0.0007
200	0.0003	0.0010
220	0.0005	0.0012
Average	0.0005	0.0010

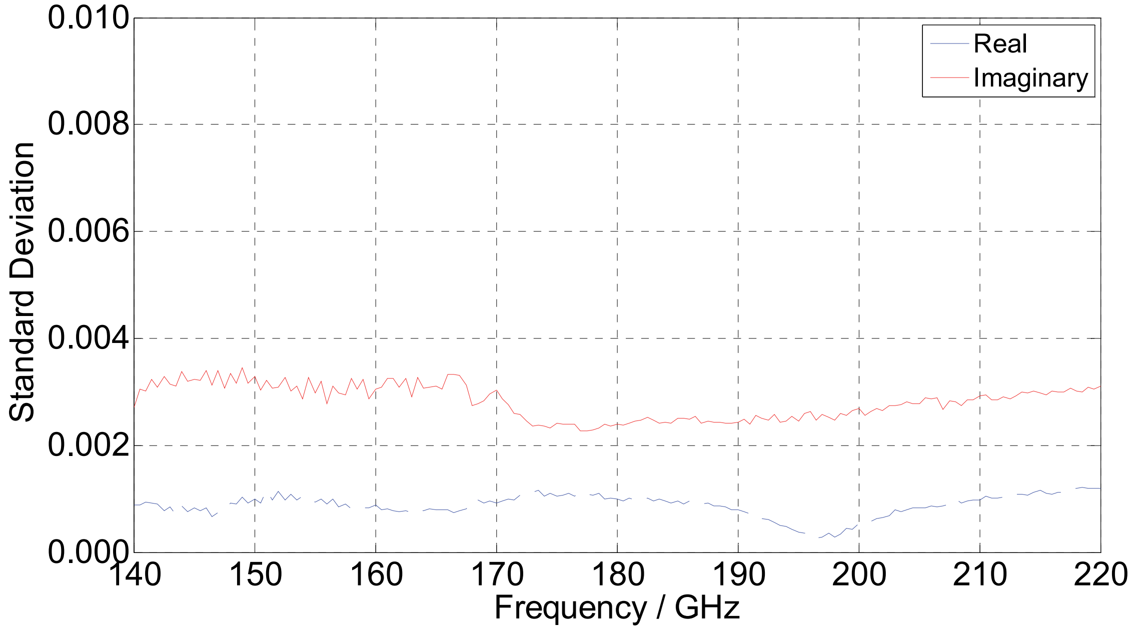

Figure 6: $s(\Gamma_R)$ **and** $s(\Gamma_I)$ **values for the mismatched termination**

Table 6: $s(\Gamma_R)$ and $s(\Gamma_I)$ values for the mismatched termination at selected frequencies

Frequency (GHz)	s(Γ_R)	s(Γ_I)
140	0.0009	0.0027
160	0.0009	0.0031
180	0.0010	0.0024
200	0.0005	0.0027
220	0.0012	0.0031
Average	0.0009	0.0028

2.4 DISCUSSION

The experimental standard deviations obtained for each DUT vary considerably depending on the type of DUT. In the case of the flush short-circuit, the experimental standard deviation does not show much variation with frequency in both real and imaginary components of the measured reflection coefficient. The same is true for the near-matched termination and the mismatched termination. The lack of variation with frequency indicates that it is appropriate to summarise the experimental standard deviations in terms of an average value obtained from the measured values at all frequencies across the waveguide band. These average values are shown in the last row in Tables 3, 5 and 6.

However, for the offset short-circuit, the experimental standard deviation varies considerably with frequency in both real and imaginary components of the measured reflection coefficient. It is therefore not considered appropriate to provide a 'frequency-independent' average value for this device, obtained from the measured values at all frequencies across the waveguide band. The variation in the experimental standard deviations is related to the phase of the reflection coefficient, as shown in Figure 7. This phase is due to the length of line used to produce the offset in the offset short-circuit. For example, as the reflection coefficient phase passes through zero degrees (at approximately 180 GHz) $s(\Gamma_R)$ is a minimum, whereas $s(\Gamma_I)$ is a maximum (see Figure 4). The ratio of $s(\Gamma_R)$ to $s(\Gamma_I)$ is close to one when the reflection coefficient phase is near to either $+45^\circ$ or -45°.

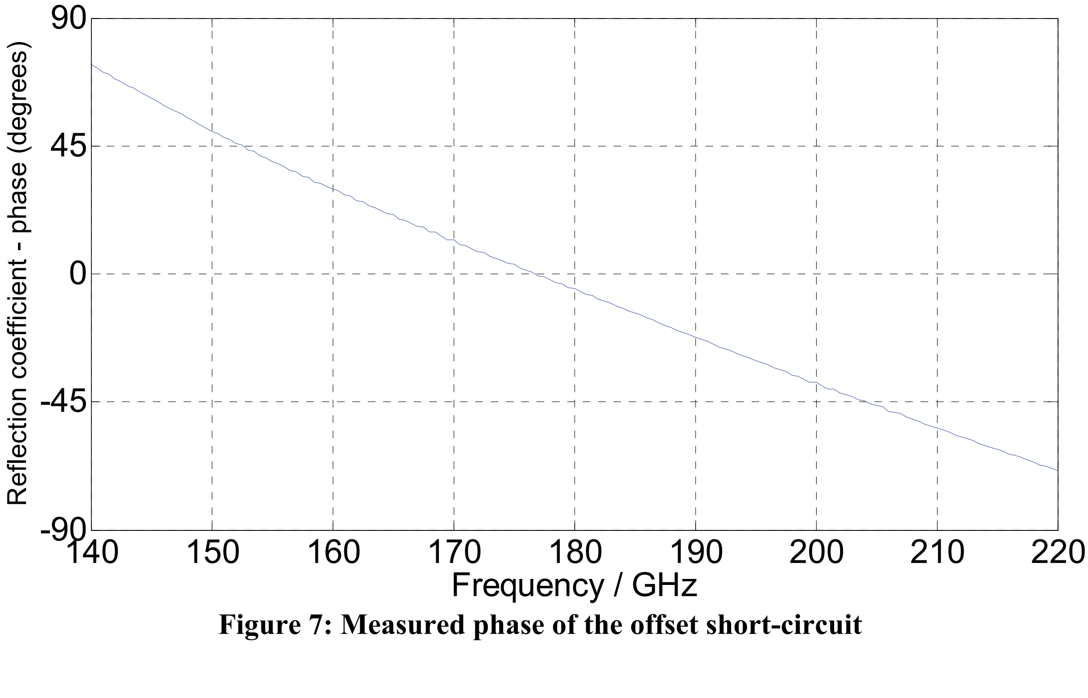

Figure 7: Measured phase of the offset short-circuit

For the flush short-circuit, $s(\Gamma_I)$ is approximately seven times larger than $s(\Gamma_R)$. For the near-matched termination, $s(\Gamma_I)$ is approximately two times larger than $s(\Gamma_R)$. For the mismatched termination, $s(\Gamma_I)$ is approximately three times larger as $s(\Gamma_R)$. In all three cases, this suggests that a shape like an ellipse could be used to enclose the scatter in these repeatability values – the size and orientation of the ellipse remains relatively constant at all frequencies across the band.

Finally, for offset short-circuit, the ratio of $s(\Gamma_I)$ to $s(\Gamma_R)$ varies considerably with frequency. Therefore, as before, this suggests that a shape like an ellipse could be used to enclose the scatter in these repeatability values – however, for this device, the size and orientation of the ellipse will vary considerably as the frequency changes. This type of behaviour has been observed elsewhere in a different waveguide band [9].

3. CALIBRATION TECHNIQUES COMPARISON

The calibration techniques being compared can be classified as either: (i) Three-Known-Loads-Thru (TKLT), (ii) Thru-Reflect-Line (TRL) or (iii) Line-Reflect-Line (LRL).

(i) TKLT calibration techniques

The calibration technique using three known loads is a traditional calibration procedure [2]-[6]. This calibration technique requires three one-port standards to be connected to both test ports of the VNA and a direct (thru) connection to be made between the test ports. One-port standards (such as a short, open and load) are used during this calibration procedure. However, in waveguide, open-circuits tend not to be used as standards because of the radiation effects at the open end of the waveguide. Therefore, an alternative form of standard is needed in waveguide. A $\lambda/4$ offset short is often used as an alternative standard for waveguide (where λ is the waveguide wavelength). The reference impedance of the entire system is set by the assumed reflection coefficients of the one-port standards.

The different possible combinations of one port standards provide different realisations of the three-known-loads calibration techniques, i.e.:

- Flush Short – $\lambda/4$ Offset Short – Load – Thru (S-OS-L-T)
- Flush Short – $\lambda/4$ Offset Short – Load – $\lambda/4$ Offset Load – Thru (S-OS-L-OL-T)
- Flush Short – $\lambda/4$ Offset Short – $\lambda/8$ Offset Short – Thru (S-OS-OS-T)

(ii) TRL calibration techniques

The TRL calibration technique [10] is widely used for precision measurement applications. This technique uses a line, a one-port reflect standard of unknown reflection at both test ports, and a direct (thru) connection as the standards. The reference impedance of the system is set by the characteristic impedance of the line. The length difference between the line and the thru should avoid $\lambda/2$ and its multiples since the computations in the calibration algorithm fail under these conditions.

This calibration technique provides accurate transmission and reflection measurements since it is usually possible to manufacture the line standard to a high degree of dimensional accuracy. It is possible to use either a single line or multiple lines for TRL calibrations. The TRL calibration techniques used in the comparison reported here are the following:

- $\lambda/4$ TRL
- $3\lambda/4$ TRL

The $\lambda/4$ TRL calibration uses only one line while the $3\lambda/4$ TRL calibration [11] uses two lines in order to obtain a phase change ranging between 210° and 330° across the full waveguide band. Each line covers only a part of the frequency range of the waveguide. However, by careful choice of line length [11], one line can be used to cover the lower part of the waveguide band, while the other line is used to cover the higher part of the waveguide band. When both lines are used together, in this way, the whole frequency range of the waveguide is covered.

(iii) LRL calibration techniques

Compared to the TRL calibration technique, the LRL calibration technique [12] replaces the thru standard of zero length with a line standard of non-zero length. The difference between the lengths of the two lines determines the effective bandwidth of the calibration procedure.

This section of the report is organised as follows: section 3.1 describes the experimental set-up; section 3.2 describes the calibration procedures used during the comparison; and, section 3.3 contains the measurement results and a discussion.

3.1 MEASUREMENT SET-UP

The measurement set-up was the same as that used for the repeatability investigation reported in Section 2. Standards from two calibration kits were used to realise the calibrations used for the calibration comparison exercise. The calibration standards used for performing the calibrations are shown in Table 7. The thru standard used in the calibration techniques was a direct connection between the test ports. The DUTs comprised a series of one- and two-port devices, as shown in Table 8.

Table 7: Calibration standards used for different calibration techniques

Calibration Techniques	**Calibration Standards**						
	VDI calibration kit (NPL reference name: CIS/C/904)				Flann Microwave calibration kit (NPL reference name: CIS/C/902)		
	Flush Short	1/4-wave Shim (0.54 mm)	1/8-wave Shim (0.27 mm)	Near-matched Termination	1.476 mm Shim	2.225 mm Shim	Thru
S-OS-L-T	✓	✓		✓			✓
S-OS-L-OL-T	✓	✓		✓			✓
S-OS-OS-T	✓	✓	✓				✓
λ/4 TRL	✓	✓					✓
3λ/4 TRL	✓				✓	✓	✓
λ/4 LRL	✓				✓	✓	

Table 8: DUTs used during the calibration comparison

Device name	Device type	Manufacturer	Serial Number
Flush Short	One-port	VDI	SC 2-54
Offset Short	One-port	Flann Microwave	177977
Near-matched Termination	One-port	Flann Microwave	177714
Mismatched Termination	One-port	Flann Microwave	177962
Waveguide Section	Two-port	Flann Microwave	221591
20dB Fixed Attenuator	Two-port	Flann Microwave	177959
625 µm Cross-connected Guide	Two-port	Flann Microwave	220500
1352 µm Cross-connected Guide	Two-port	Flann Microwave	220498

3.2 CALIBRATION PROCEDURE

The sequence of calibrations followed a set procedure: (i) after performing each calibration, the calibration data (i.e. the coefficients in the error terms) was saved to the VNA; (ii) each DUT was then connected to the VNA and its data corrected with respect to each set of calibration data. This procedure was adopted in order to avoid additional errors due to DUT connection repeatability. Also, as a consequence, the same set of raw DUT data has been corrected with respect to each set of calibration data.

For the DUTs that comprised simple sections of line (i.e. the offset short and the waveguide section) the measured phase (of the reflection coefficient, for the offset short, and, the transmission coefficient, for the waveguide section) has been used to calculate the 'electrical' length following the techniques described in [13]. The electrical length calculations were then compared with a 'mechanical' length made using dimensional measurement techniques.

For an offset short, the phase, θ, of the measured reflection coefficient (in degrees) is related to the offset length, l, (in metres) as follows:

$$l = \frac{180 + 360n - \theta}{2\beta_g} \tag{6}$$

where β_g is the guide phase constant (in degrees per metre) and n is an integer (n = 0, 1, 2, 3, ...). The choice for the value of n is made by finding a length that is within a given tolerance of the expected length of the offset short.

For a waveguide section, the phase, θ, of the measured transmission coefficient (in degrees) is related to the electrical length l (in metres) as follows:

$$l = \frac{360n - \theta}{\beta_g} \tag{7}$$

where β_g is the guide phase constant (in degrees per metre) and n is an integer (n = 0, 1, 2, 3, ...). As before, the choice of value for n is made by finding a length that is within a given tolerance of the expected length of the waveguide section.

3.3 MEASUREMENT RESULTS AND DISCUSSION

The measurement results for reflection coefficient magnitudes are presented using a linear scale, while the transmission coefficient magnitudes are presented using a dB scale. The following calibration techniques were used (see Table 7):

- Flush Short – $\lambda/4$ Offset Short – Load – Thru (S-OS-L-T)
- Flush Short – $\lambda/4$ Offset Short – Load – $\lambda/4$ Offset Load – Thru (S-OS-L-OL-T)
- Flush Short – $\lambda/4$ Offset Short – $\lambda/8$ Offset Short – Thru (S-OS-OS-T)
- Thru – Reflect – $\lambda/4$ Line (TRL)
- Thru – Reflect – $3\lambda/4$ Line (TRL)
- $3\lambda/4$ Line1 – Reflect – $3\lambda/4$ Line2 (LRL)

3.3.1 One-port Measurements

The measurements of the magnitude of the reflection coefficient for the one-port DUTs (flush short, offset short, near-matched termination and mismatched termination) are shown in Figures 8 to 11.

In principle, no passive device can have a linear reflection coefficient magnitude that is greater than unity. However, from Figures 8 and 9, it is clear that some of the measured linear reflection coefficient magnitude values for the flush short and offset short are greater than one. This is likely due to systematic errors in the VNA that have not been correctly (or fully corrected) by the calibration procedures.

The near-matched termination results, presented in Figure 10, show that the S-OS-OS-T calibration results exhibit higher values than results produced with respect to the other calibration techniques. This could be caused by the S-OS-OS-T calibration technique not using a calibration standard whose reflection coefficient is near to the centre of the reflection coefficient plane (i.e., a near-matched load standard). The measurements of the reflection coefficient magnitude of the mismatched termination, presented in Figure 11, indicate a value of around 0.5. Generally, there is good agreement between the results for this mismatch when measured with respect to the different calibration techniques.

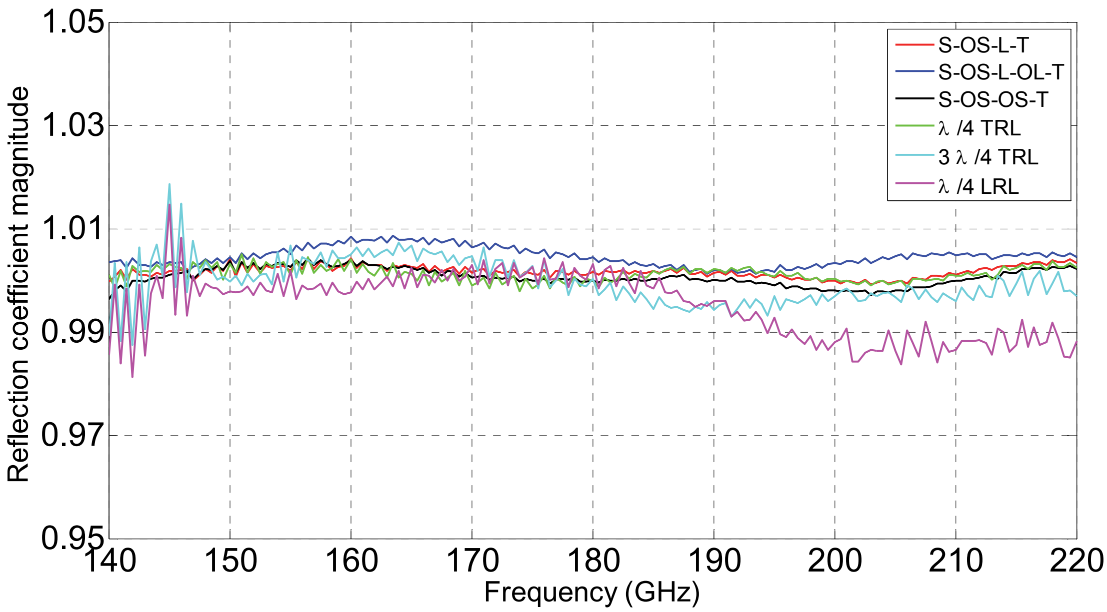

Figure 8: Measurements of the reflection coefficient magnitude of a flush short

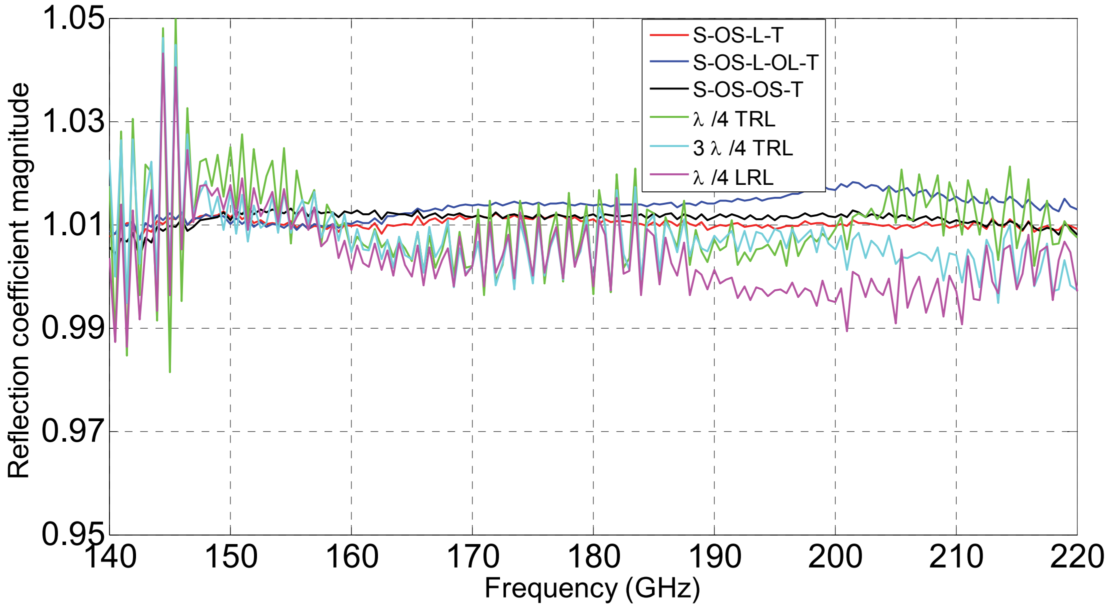

Figure 9: Measurements of the reflection coefficient magnitude of an offset short

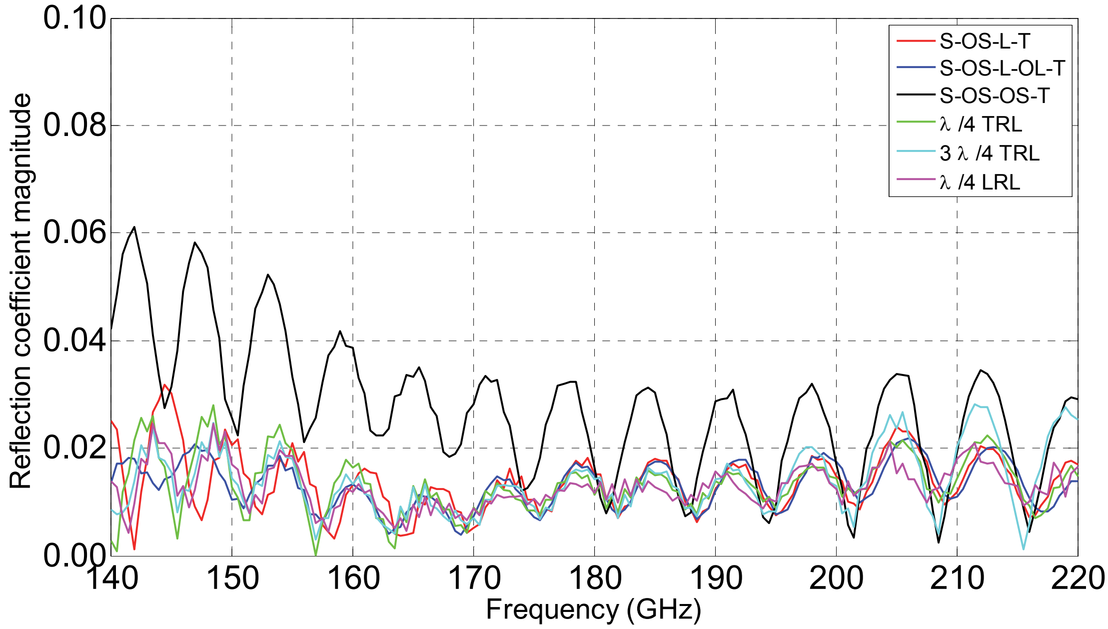

Figure 10: Measurements of the reflection coefficient magnitude of a near-matched termination

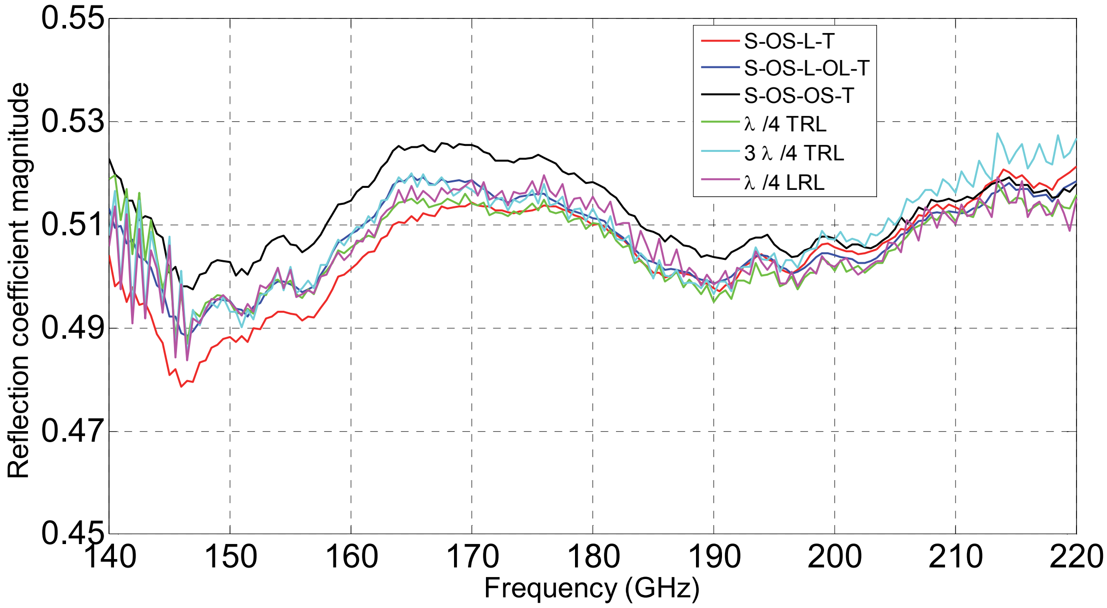

Figure 11: Measurements of the reflection coefficient magnitude of a mismatched termination

3.3.2 Two-port Measurements

The two port DUTs were a waveguide section, a fixed 20 dB precision attenuator and two cross-connected waveguides of different lengths [14]. The results obtained using the different calibrations are shown in Figures 12 to 20.

The transmission coefficient magnitude and phase measurements of the waveguide section, with nominal length 35 mm, are shown in Figures 12 and 13. The different calibrations agree well with each other, for both the magnitude and phase measurements, except for the $\lambda/4$ LRL calibration which shows lower values for the transmission coefficient magnitude in the upper half of the frequency band. The attenuation constant, in dB per millimetre (dB/mm), of the waveguide section with nominal length 35 mm, is also shown in Figure 14. The attenuation constant provides an indication of the measured loss per unit length. For a lossless line the attenuation constant is 0 dB/mm. However, from Figure 12, measurements of the waveguide section clearly indicate transmission losses. Figure 14 shows that the attenuation constant varies from 0.016 dB/mm to 0.008 dB/mm over the whole waveguide band.

The fixed precision attenuator transmission coefficient measurements are presented in Figures 15 and 16. The transmission measurements suggest that the attenuator is a 20 dB attenuator. Both magnitude and phase measurements show that the different calibrations show good agreement.

Two cross-connected waveguide devices of different lengths were also measured. A ‘cross-guide’ is a waveguide section that is connected in such a way that the waveguide aperture is at right angles to the usual connection orientation of a waveguide. The electromagnetic wave decays exponentially as it moves through the cross-guide section. As the length of the cross-guide gets longer, more attenuation is produced. Therefore, a cross-connected section of waveguide can be considered as a primary standard of attenuation in any waveguide size [14]. They can be especially useful in the ‘small’ waveguide sizes where waveguide verification devices and currently not available. The measured magnitude and phase of the transmission coefficients for the two sections of cross-guide (of lengths 625 μm and 1352 μm) are presented in Figures 17 to 20. These Figures show good agreement between the different calibration techniques, for both the magnitude and phase measurements. It can also be seen from the Figures 17 and 19 that the longer length cross-guide (of 1352 μm) provides greater attenuation than the shorter length cross-guide (of 625 μm).

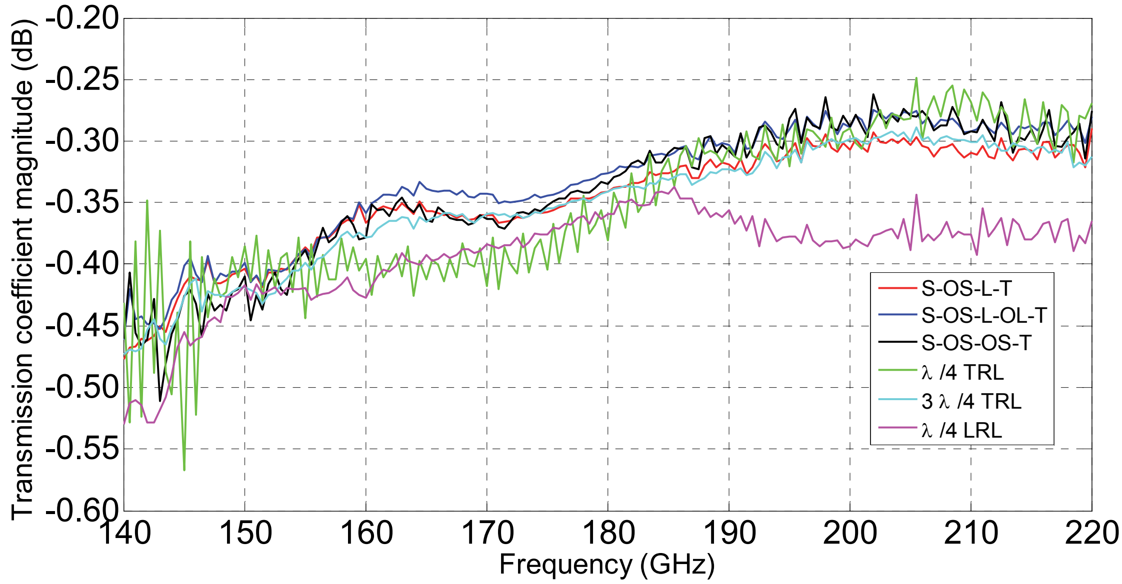

Figure 12: Measurements of the transmission coefficient magnitude of a waveguide section of 35 mm nominal length

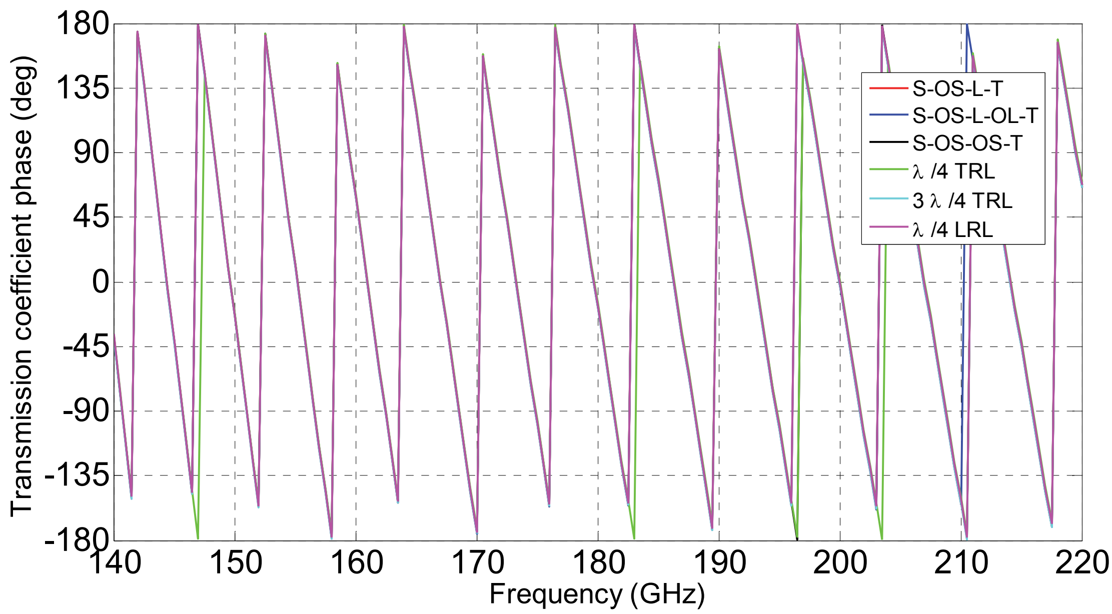

Figure 13: Measurements of the transmission coefficient phase of a waveguide section of 35 mm nominal length

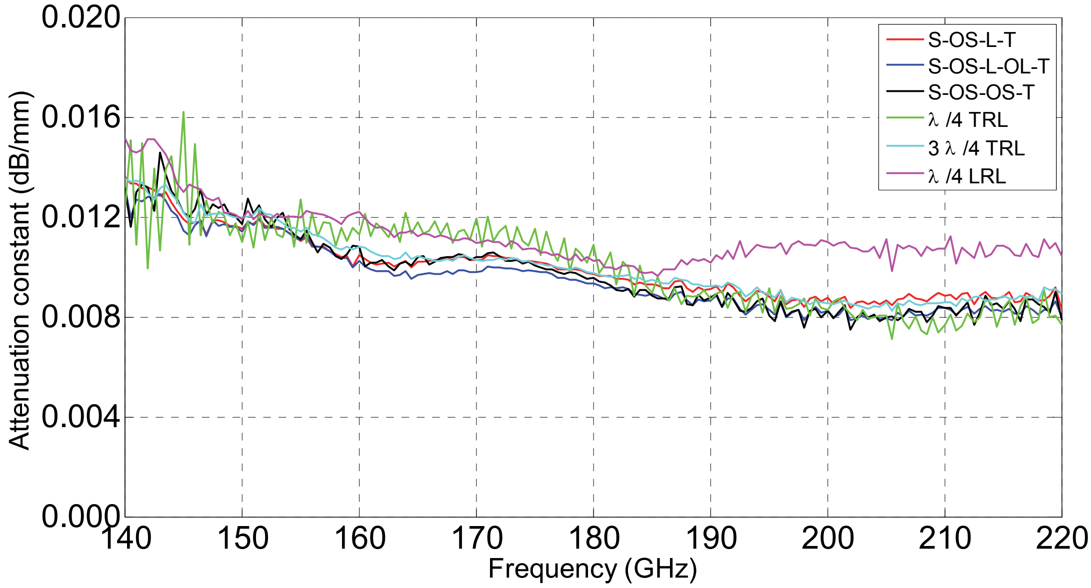

Figure 14: Measured attenuation constant of a waveguide section of 35 mm nominal length

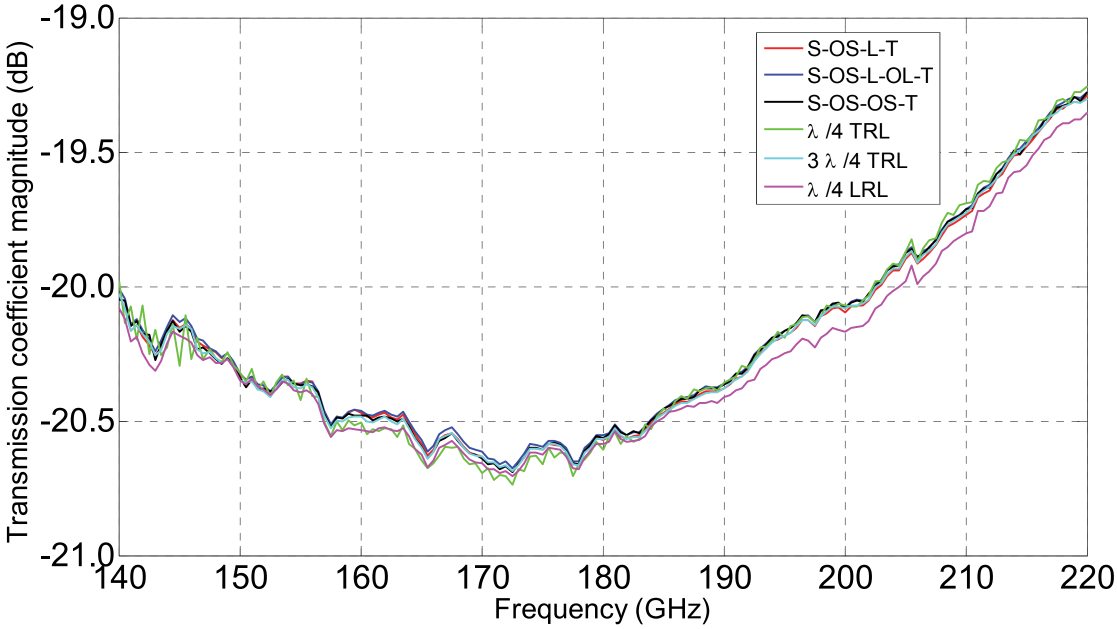

Figure 15: Measurements of the transmission coefficient magnitude of a fixed precision attenuator of 20 dB nominal value

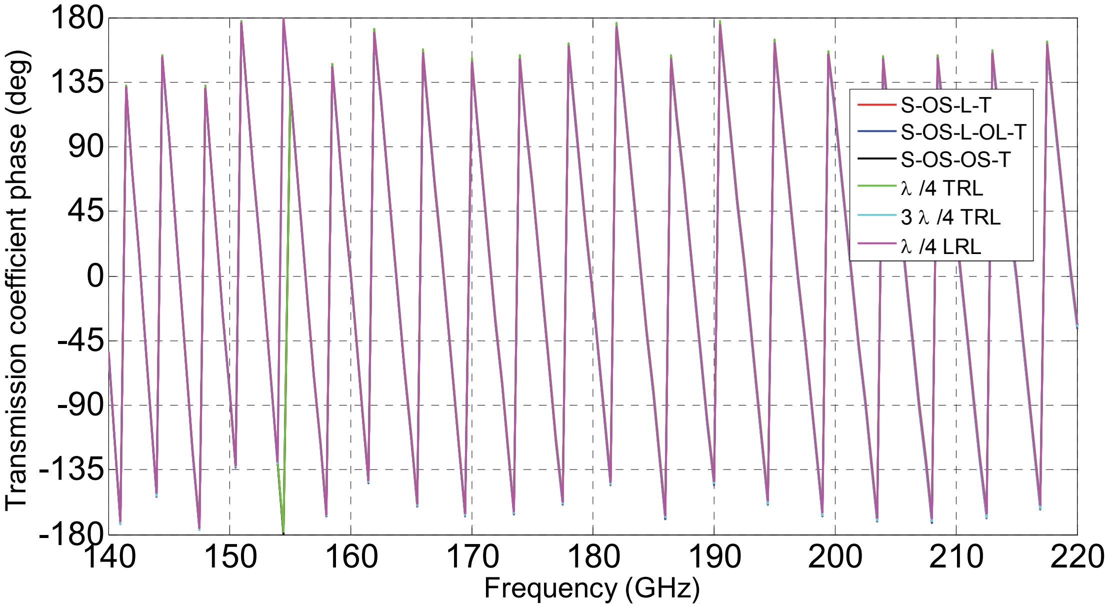

Figure 16: Measurements of the transmission coefficient phase of a fixed precision attenuator of 20 dB nominal value

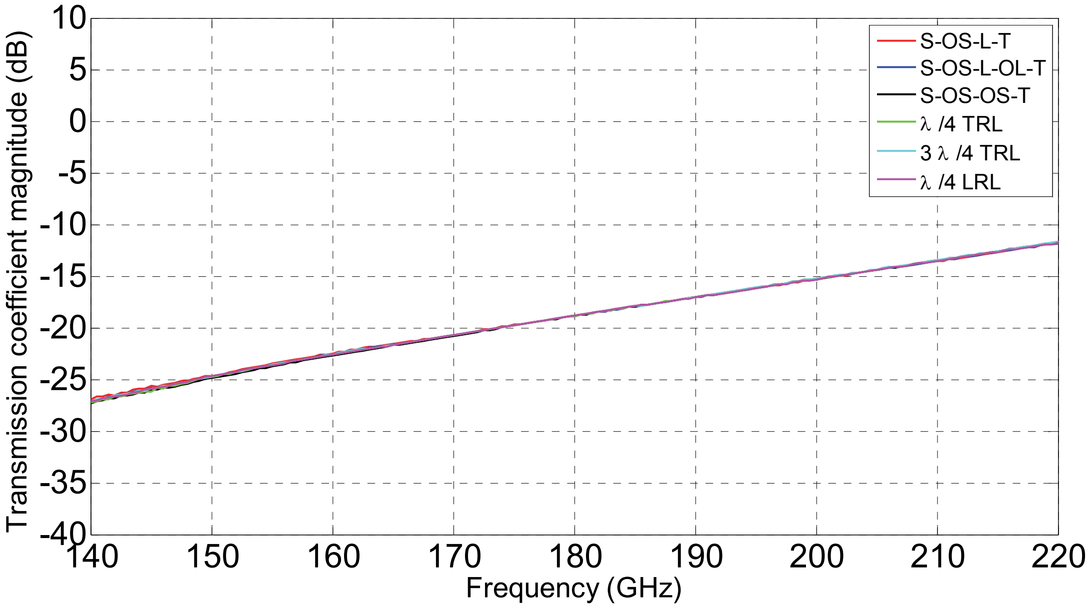

Figure 17: Measurements of the transmission coefficient magnitude of a 625 µm length cross-guide

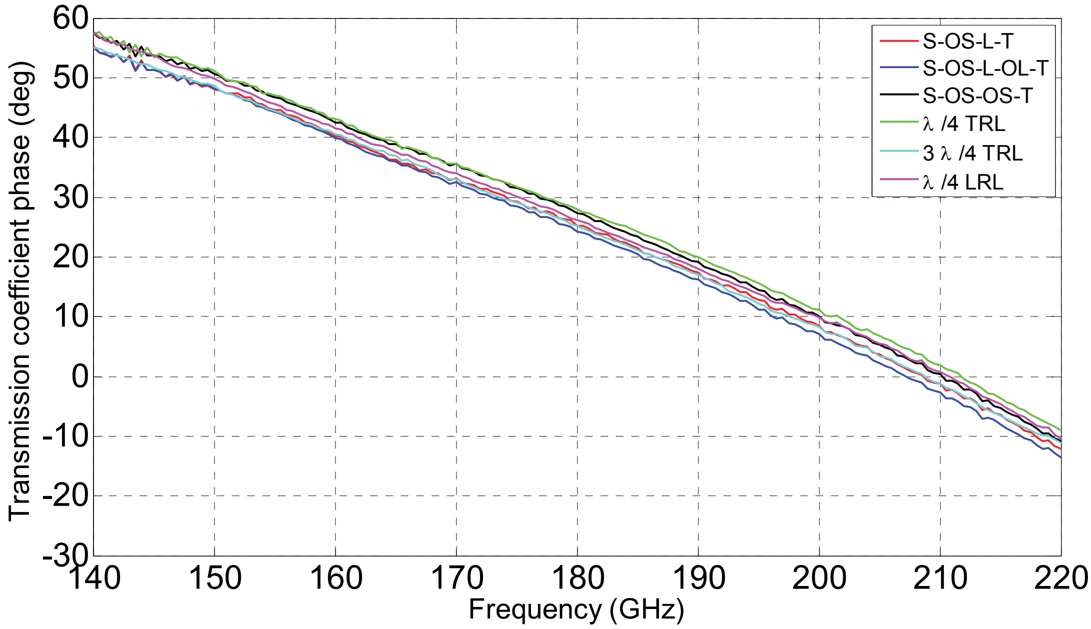

Figure 18: Measurements of the transmission coefficient phase of a 625 µm length cross-guide

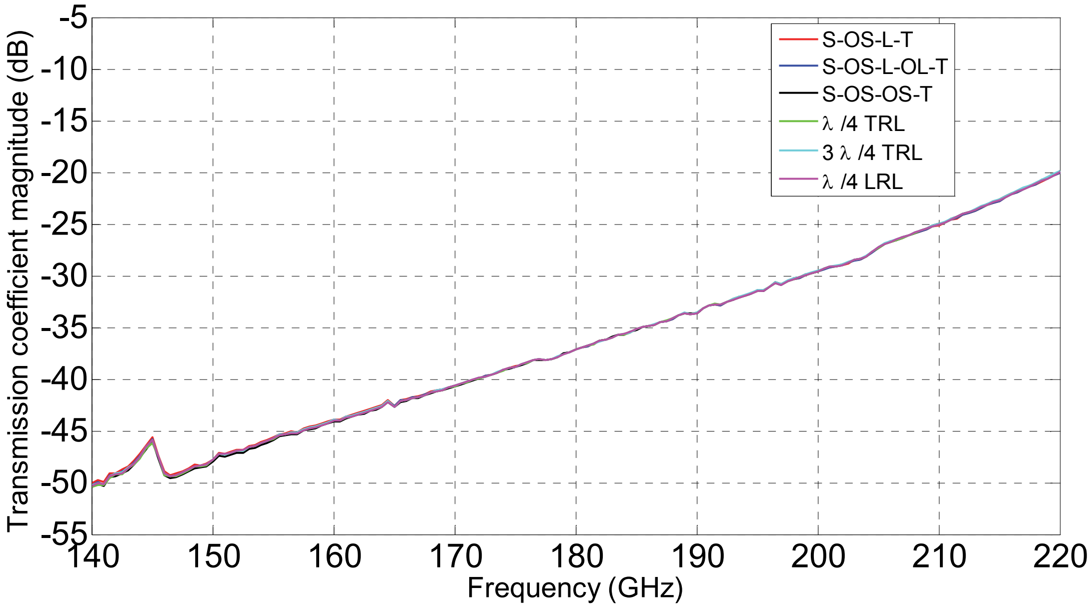

Figure 19: Measurements of the transmission coefficient magnitude of the 1352 µm length cross-guide

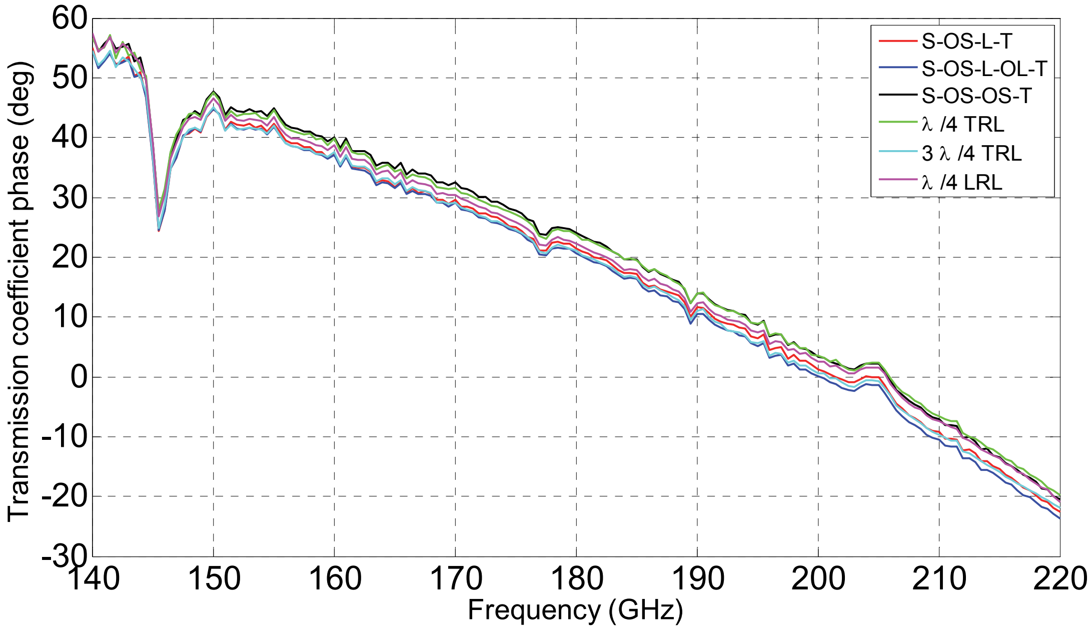

Figure 20: Measurements of the transmission coefficient phase of a 1352 µm length cross-guide

3.3.3 Length Analysis

The electrical lengths for the offset short and the waveguide section have also been computed using the reflection and transmission phase measurements, respectively. These length computations have then been compared with a mechanical length determination. This is shown in Figure 21 (for the offset short) and Figure 22 (for the waveguide section). The electrical length for the offset short was computed using equation (6), while equation (7) was used to compute the length for the waveguide section, for each calibration technique. The mechanical length measurements for both DUTs were also made at NPL. The length for the offset short was measured optically while the length of the waveguide section was measured using a digital vernier calliper. Both electrical and mechanical length determinations are presented in Figures 21 and 22, for comparison purposes.

It can be seen, from Figure 21, that the electrical length determinations for the offset short, using the different calibration techniques, show reasonable agreement (generally, to within 10 µm across the full waveguide band) with the mechanical length determination. However, the electrical determinations generally produce longer length values compared to the mechanical determination.

On the other hand, the electrical length determinations for the waveguide section are significantly different from the mechanical determination, especially at the lower end of the frequency range, as shown in Figure 22. This is likely due to the attenuation losses (i.e. non-zero attenuation constant) in the waveguide section causing an increase in the guided phase constant from its lossless value by an amount that is frequency dependent [13]. It can be seen, from Figure 23, that the estimated value of phase constant ($\beta_{estimated}$) obtained using the transmission losses is higher than the lossless phase constant ($\beta_{lossless}$). The phase constant difference ($\Delta\beta$) is also frequency dependent. However, the electrical lengths obtained using different calibration techniques are very similar. As with the measurements of the offset short, the electrical length determination of the waveguide section produces longer length values compared to the mechanical determination.

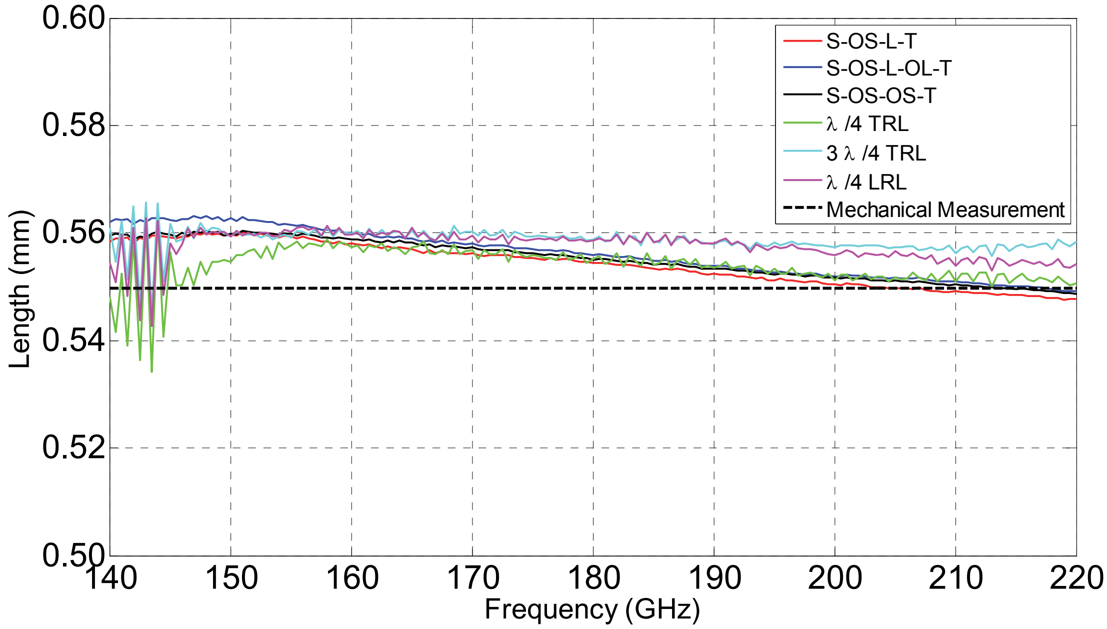

Figure 21: Length computations for an offset short

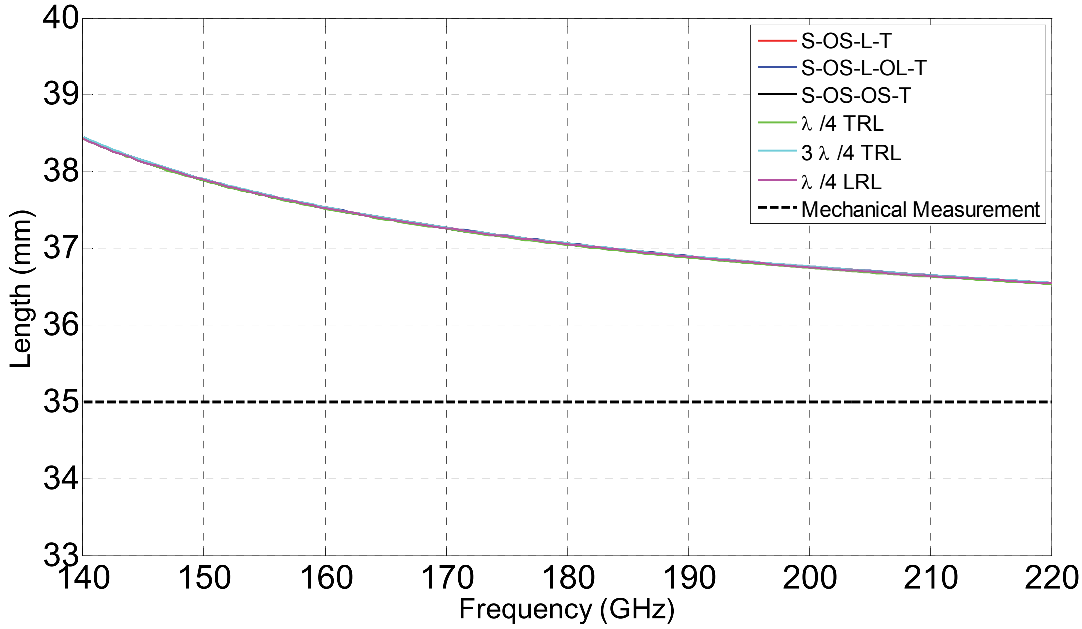

Figure 22: Length computations for a 35 mm waveguide section

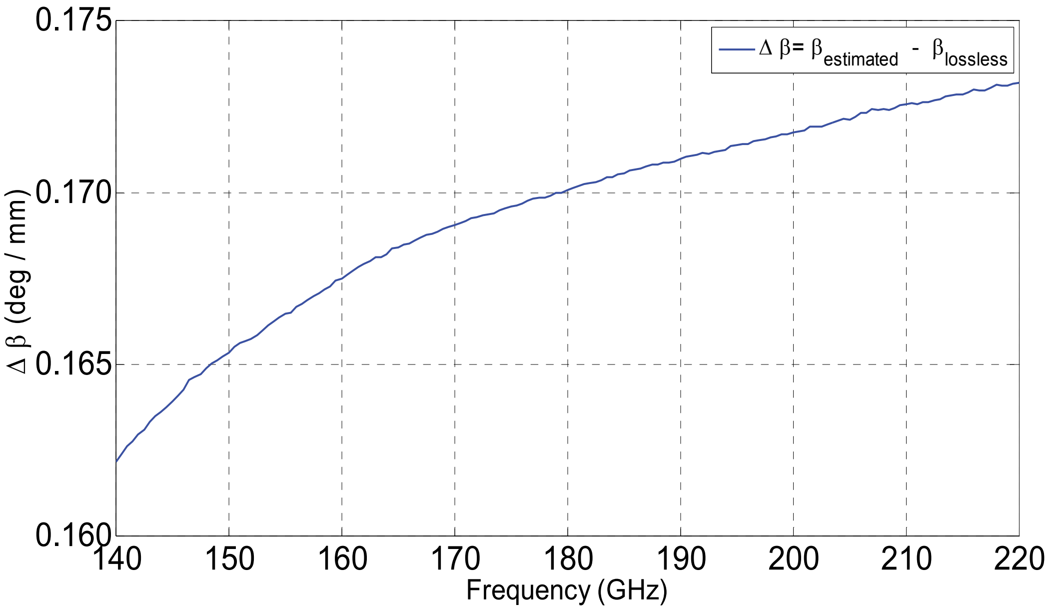

Figure 23: Phase constant difference (Δβ) for a 35 mm waveguide section

4. CONCLUSION

This report has presented the results from two investigations that form part of the commissioning of the new NPL 140 GHz to 220 GHz Vector Network Analyser measurement system. These investigations were: (a) connection repeatability; and (b) comparison of calibration techniques. The purpose of this commissioning activity was to benchmark the performance of this new NPL facility for providing S-parameter measurements of one- and two-port devices in the WR-05 waveguide size.

Four DUTs were used in the connection repeatability investigation: a flush short-circuit, an offset short-circuit, a near-matched termination and a mismatched termination. The repeatability analysis was based on calculations of the experimental standard deviation of the repeated measurements at each frequency for each DUT in order to establish the variability in the measurement data. This analysis was performed separately for both the real and imaginary components of the measured complex-valued linear reflection coefficient. Typical values of experimental standard deviation observed for each DUT were: ≤ 0.002 for the near-matched termination; ≤ 0.004 for the mismatched termination; ≤ 0.008 for the offset short-circuit; ≤ 0.010 for the flush short-circuit.

The S-parameter results obtained using different two-port calibration techniques showed relatively good agreement between the different calibration techniques. At some frequencies (particularly below 150 GHz), the magnitude of the linear reflection coefficient values for the flush short-circuit and the offset short-circuit showed values that were greater than unity. This is due to systematic errors in the VNA that remain after the calibration process. This requires further investigation to see if the effects due to these systematic errors can be reduced in some way.

The computations of electrical length for the two-port waveguide section were found to be substantially different from the mechanical measurement of the waveguide section, especially at the lower end of the frequency range. This is likely due to the attenuation losses that were observed in measurements of the waveguide section causing an increase in the waveguide phase constant value from its lossless value by an amount that is frequency dependent. This requires further investigation to see if this effect can be compensated for in electrical determinations of the length of these waveguide sections.

A next step in the further investigation of the performance of this new facility will be an evaluation of the uncertainty in S-parameters measurements made using the system. This will involve an investigation into the various sources of uncertainty, including the definitions of the calibration standards, VNA noise, repeatability and overall system drift.

5. ACKNOWLEDGEMENTS

The work described in this report was funded through the European Metrology Research Programme (EMRP) Project SIB62 'Metrology for New Electrical Measurement Quantities in High-frequency Circuits'. The EMRP is jointly funded by the EMRP participating countries within EURAMET and the European Union.

Nosherwan Shoaib's involvement with this work was funded through the *Lifelong Learning Programme (LLP)/ERASMUS Placement* by Politecnico Di Torino, Italy.

6. REFERENCES

[1] JCGM 200:2012, "International vocabulary of metrology – basic and general concepts and associated terms", Third Edition, 2012. Available at: www.bipm.org.

[2] W. Kruppa and K.F. Sodomsky, "An explicit solution for the scattering parameters of a linear two-port measured with an imperfect test set", *IEEE Trans. Microwave Theory Tech.*, vol. MTT-19, no. 1, pp. 122-123, 1971.

[3] S. Rehnmark, "On the calibration process of automatic network analyzer systems", *IEEE Trans. Microwave Theory Tech.*, vol. MTT-22, no. 4, pp. 457-458, 1974.

[4] G. F. Engen, "Calibration technique for automated network analyzers with application to adapter evaluation", *IEEE Trans. Microwave Theory Tech.*, vol. MTT-22, pp. 1255-1260, 1974.

[5] N. R. Franzen and R. A. Speciale, "A new procedure for System Calibration and error removal in automated S-parameter measurements", *Proc. 5th European Microwave Conf.*, pp. 69-73, 1975.

[6] J. Fitzpatrick, "Error models for system measurement", *Microwave Journal*, vol.21, pp.63-66, May 1978.

[7] JCGM 100:2008, "Evaluation of measurement data-Guide to the expression of uncertainty in measurement", First Edition, September 2008. Available at: www.bipm.org.

[8] N. M. Ridler, R. G. Clarke, M. J. Salter and A. Wilson, "Traceability to national standards for S-parameter measurements in waveguide at frequencies from 140 GHz to 220 GHz", in *Proc. 76th ARFTG Microwave Measurement Conference*, pp. 1-7, Dec. 2010.

[9] N. M. Ridler and R. G. Clarke, "Investigating Connection Repeatability of Waveguide Devices at Frequencies from 750 GHz to 1.1 THz" *Proc. 82nd ARFTG Microwave Measurement Conference*, pp. 87-99, Nov. 2013.

[10] G. F. Engen and C. A. Hoer, "Thru-reflect-line: An improved technique for calibrating the dual six port automatic network analyzer", *IEEE Trans. Microwave Theory Tech.*, vol. MTT-27, pp. 987-993, Apr. 1979.

[11] N. M. Ridler, "Choosing line lengths for calibrating waveguide vector network analyzers at millimetre and sub-millimetre wavelengths", *NPL Report TQE 5*, pp. 1-21, Mar. 2009.

[12] C. A. Hoer and G. F. Engen, "On-line accuracy assessment for the dual six-port ANA: extension to nonmating connectors", *IEEE Trans. Instrumentation & Measurement*, vol. IM-36, No 2, pp. 524-529, June 1987.

[13] S. Protheroe and N. Ridler, "Using air lines as references for VNA phase measurements", *Proc. ARMMS Conference*, Newport Pagnell, Buckinghamshire, 7th and 8th Nov. 2005.

[14] N. M. Ridler and M. J. Salter, "Cross-connected waveguide lines as standards for millimeter- and submillimeter-wave vector network analyzers", *Proc. 81st ARFTG Microwave Measurement Conference,* pp. 1-7, June 2013.

APPENDIX: ADDITIONAL DATA ANALYSIS

This appendix presents an alternative method (from [8]) for calculating the experimental standard deviation in the complex-valued linear reflection coefficient. Values obtained using this method have been calculated for the near-matched termination and offset short-circuit used during the investigation described in this report, and these values are compared with values found elsewhere [8].

For this alternative method, the experimental standard deviation, $s(|\Gamma|)$, is defined as:

$$s(|\Gamma|) = \sqrt{\frac{1}{n-1}\sum_{m=1}^{n} |\Gamma_m - \overline{\Gamma}|^2} \qquad (8)$$

where n is the number of repeated measurements (here, n = 10), $\overline{\Gamma}$ is the mean complex-valued reflection coefficient (using equations (2) and (4)) and the Γ_m (where m = 1 to n) are the repeated measurements of the complex-valued reflection coefficient.

Values for $s(|\Gamma|)$, for the near-matched termination and offset short-circuit, along with values presented in [8], are shown in Table 9.

Table 9: $s(|\Gamma|)$ values, obtained using equation (8), for the near-matched termination and the offset short-circuit at selected frequencies

Frequency (GHz)	Near-matched termination	Near-matched termination [8]	Offset short-circuit	Offset short-circuit [8]
140	0.001 0	0.002 7	0.007 0	0.006 0
150	0.001 0	0.002 2	0.008 1	0.005 8
160	0.001 3	0.002 4	0.007 5	0.005 9
170	0.000 6	0.001 4	0.007 2	0.006 7
180	0.000 9	0.002 1	0.007 0	0.007 4
190	0.001 7	0.003 1	0.005 9	0.008 6
200	0.001 0	0.001 8	0.004 6	0.009 0
210	0.001 2	0.002 9	0.003 7	0.010 5
220	0.001 3	0.001 7	0.002 3	0.009 8

The values for $s(|\Gamma|)$ for the near-matched termination and offset short-circuit reported in [8] were obtained using a different measurement system from that used for the measurements described in this report. The measurement data reported in [8] was collected using a Hewlett Packard 8510 VNA with Oleson Microwave Labs (OML) millimetre-wave extender heads. However, it can be seen from Table 9 that the values for $s(|\Gamma|)$ in both cases (i.e. the values given in this report and values reported in [8]) are approximately of the same order. For the values given in this report, the $s(|\Gamma|)$ values for the near-matched termination remain fairly constant with frequency, whereas the $s(|\Gamma|)$ values for the offset short-circuit decrease as the frequency increases.